Substituent Effect of *N*,*N*-Dialkylamides on the Intermolecular Hydrogen Bonding with Thioacetamide

Nak-Kyoon Kim,[†] Ho-Jin Lee,[†] Kee-Hyun Choi,[†] Jeong-A Yu,[‡] Chang-Ju Yoon,[§] Jeunghee Park,*[,||] and Young-Sang Choi*[,†]

Department of Chemistry, Korea University, 1 Anam-dong, Seoul, S. Korea 136-701, Department of Science Education, Chosun University, Kwangju, S. Korea 501-759, Department of Chemistry, The Catholic University of Korea, Pucheon, S. Korea, 420-743, and Department of Chemistry, Korea University, Jochiwon, Chungnam, S. Korea 339-700

Received: November 17, 1999; In Final Form: March 24, 2000

The alkyl substituent effect on the intermolecular hydrogen-bonding properties of tertiary amides has been investigated experimentally and theoretically. *N*,*N*-Dimethylformamide (DMF), *N*,*N*-diethylformamide (DEF), *N*,*N*-diisopropylformamide (DIF), *N*,*N*-dimethylacetamide (DMA), *N*,*N*-diethylacetamide (DEA), and *N*,*N*-diisopropyl acetamide (DIA) were chosen as proton acceptors for thioacetamide (TA) in CCl_4 solution. Thermodynamic parameters for the interaction of tertiary amides with TA have been measured by near-infrared (NIR) absorption spectroscopy. For DMF, DEF, and DIF, the standard enthalpy change of 1:1 hydrogen-bonded complex formation is about −19.5 kJ/mol and the equilibrium constant at 298 K is about 60 M^{-1}. For DMA, DEA, and DIA, the standard enthalpy change increases from −18.9 to −19.8 kJ/mol and the equilibrium constant at 298 K decreases from 65 to 50 M^{-1}, as the alkyl group becomes bulky. The IR data of N−H stretching vibrations of TA are very consistent qualitatively with the NIR thermodynamic data. The temperature dependence of proton NMR chemical shift has been examined for N−Hs of TA to understand the characteristics of hydrogen bonding. We suggest that more hydrogen-bonding interaction via the hydrogen syn to the sulfur atom of TA could take place in the formamide series, compared to the acetamide series. The proton affinity of these tertiary amides is calculated by using HF/6-31+G*, HF/6-31G**, and B3LYP/6-31G** levels of ab initio molecular orbital theory.

1. Introduction

Polypeptides are usually inherently flexible, but they adopt a compact and highly ordered conformation to perform the biological functions. The conformation is constrained by maximum binding energy interactions between the peptide linkages in either hydrophilic or hydrophobic environments. To understand many factors determining the polypeptide structure, simple amide systems have been investigated extensively for many years.[1−10]

A number of experimental and theoretical works have focused on the formation of amide−amide hydrogen bonds, but the alkyl effect on the intrinsic binding energy between N−H and C═O groups is still not completely understood. Le Questel et al. measured the complex formation constant of 4-fluorophenol with secondary and tertiary amides, showing a greater decrease with the alkyl substituents on the carbonyl carbon than on the nitrogen.[2] Hansen and Swenson reported the thermodynamic parameters for H_2O−amide hydrogen-bonding formation in CCl_4.[3] For I_2−amide complex formation in CCl_4, the equilibrium constant and thermodynamic data were measured by Drago et al.[4] These data were simply explained by using inductive and steric effects of alkyl substituents. However, Wolfenden studied the solvation free energy of highly polar amides in water and suggested a nonadditive effect by the methyl group substituted on the nitrogen.[5] Morganiti and Kollman reported that theoretical solvation free energy increases monotonically with the methyl addition.[6]

For a series of simple amides, the rotational barrier around the C−N bond in the gas phase has been recently investigated, showing that the rotational barrier decreases as the size of alkyl substituent increases and is less affected by the substituent on the N-site than by that on the C-site of the carbonyl group.[7−14] The rotational barrier of thioamide was found to be higher than that of amide, by experiments and theoretical calculations.[15−19] These results cannot be explained simply by using the electronegativity or steric effects of substituents.

In this paper, we have explored the alkyl substituent effect on the intermolecular hydrogen-bonding formation between thioacetamide (TA) as a proton donor and tertiary amide as a proton acceptor in a nonpolar solvent, CCl_4, by using near-infrared (NIR), infrared (IR), and proton (^1H) nuclear magnetic resonance (NMR) spectroscopic techniques. Tertiary amides are six symmetrical *N*,*N*-dialkyl-substituted amides such as *N*,*N*-dimethylformamide (DMF), *N*,*N*-diethylformamide (DEF), *N*,*N*-diisopropylformamide (DIF), *N*,*N*-dimethylacetamide (DMA), *N*,*N*-diethylacetamide (DEA), and *N*,*N*-diisopropylacetamide (DIA). The NIR spectroscopic technique has provided very accurate measurements of the thermodynamic parameters for the hydrogen-bonding formation of TA with various proton acceptors.[21−23] The temperature dependence of the chemical shifts of the amide proton has been widely used as a tool for studying the hydrogen bond of peptides.[25,26] It is known that the intermolecular hydrogen-bonded amide protons can display a large temperature

* Corresponding authors. E-mail: yschoi@kuccnx.korea.ac.kr. E-mail: parkjh@tiger.korea.ac.kr.
[†] Korea University, Seoul.
[‡] Chosun University.
[§] The Catholic University of Korea.
[||] Korea University, Chungnam.

10.1021/jp994092u CCC: $19.00
Published on Web 05/18/2000

dependence of the chemical shift relative to the free amide protons in a nonpolar solvent. Therefore, the chemical shift and its temperature dependence could be correlated with the thermodynamic data of TA−amide hydrogen bonding. To compare with the experimental results, we have calculated ab initio proton affinity (PA) values for these tertiary amides.

2. Experimental Section

2.1. Reagent and Sample Preparation. Thioacetamide (TA) (Aldrich, 99%) was dried at room temperature under a reduced pressure for 24 h and stored in a nitrogen-filled glovebox. DMF (Aldrich, 99%), DEF (Aldrich, 99%), DIF (Aldrich, 98%), DMA (Aldrich, 99.8%), DEA (Merck, 97%), DIA (Aldrich, 99%), and CCl_4 (J. T.Baker, HPLC grade) were dried by adding 4 Å molecular sieves (Aldrich) without further purification. Because of low solubility (∼10 mM) of TA in CCl_4, we prepared a concentrated stock solution by mixing TA with tertiary amides in CCl_4 and diluted it by adding CCl_4. The molar concentration ratio of TA (2.7−8 mM) to tertiary amides was 1:5. All samples were prepared in a nitrogen-filled glovebox.

2.2. Instruments. *Near-IR and IR Spectroscopy.* The NIR absorption spectrum of TA/amide/CCl_4 solution was measured by using a Cary 5G UV−VIS−NIR spectrophotometer (Varian Inc.). The 1-cm path length quartz cells were used. Since we studied the NIR absorption band of TA, the absorption due to the amide and CCl_4 was eliminated by placing a matching cell containing an equal amount of the amide in the path of the reference beam. The sample and reference cells were placed in a multicell holder (Varian Inc.) connected to a constant temperature controller (Varian Inc.). The temperature range was 278−328 K, and temperature fluctuation during the measurement was less than ±0.1 K. The cell compartment was purged by nitrogen gas passing through calcium chloride, to remove the humidity. The baseline was always checked before the measurement. The Peak Fit (AISN Software Inc.) program was used for the nonleast-squares fit of the NIR absorption band by a Gaussian−Lorentzian product function. The program terminates its iteration when χ^2 was less than 1×10^{-7}.

NMR Spectroscopy. Proton (^{1}H) NMR measurements as a function of temperature (283−313 K) were performed by using a Varian Unity plus 600 spectrometer which operates at 599.7 MHz. Field homogeneity was optimized by using $CDCl_3$. No field lock was used during the data acquisition. The sample was equilibrated for 20−30 min at a set temperature and then the NMR spectrum accumulated 256 times. Tetramethylsilane (TMS) was used as a reference for all chemical shifts. The cell temperature was measured by using a thermocouple gauge located inside the probe compartment and checked by measuring the chemical shifts of pure methanol. The temperature deviation was less than 1 K. The resolution of the ^{1}H NMR spectrum was 0.4577 Hz.

2.3. Computations. Computations were carried out using the Gaussian 94W program[27] operated on a Pentium II 400 MHz PC. All possible geometries for the tertiary amides were examined by using the AM1 semiempirical method,[28] and then the most stable conformer was selected. The geometry of stable conformer was fully optimized at the HF/6-31+G*, HF/6-31G**, and B3LYP/6-31G** levels.[29,30]

Proton affinity (PA) is defined as the negative value of enthalpy change for the $B(g) + H^+(g) \rightarrow BH^+(g)$ reaction. For evaluation of the absolute PA value, the following equation was used:[15]

$$PA(B) = -\Delta E^\circ_{elec} - \Delta ZPE + \Delta E_{vib}(T) + 5/2RT$$

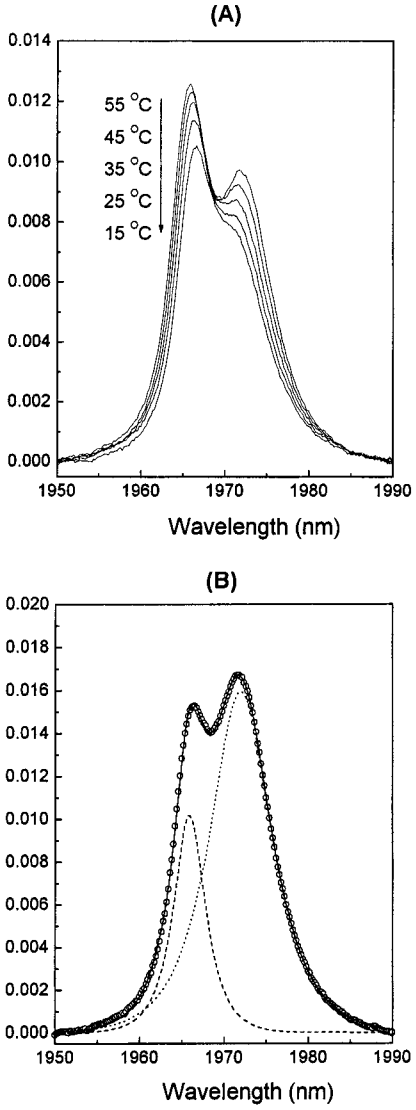

Figure 1. (A) The ν^{as}_{N-H} + Amide II combination band of 8.0 mM TA with 40.0 mM DMA in CCl_4 at various temperatures, showing an isosbestic point. (B) Computer-resolved ν^{as}_{N-H} + amide II band of 4.6 mM TA with 27.8 mM DMA in CCl_4, at 298 K. Filled circles (●), dashes (---), and dots (•••) represent the measured absorption spectrum, the resolved monomeric band, and the hydrogen-bonded band, respectively.

Here ΔE°_{elec} represents the difference between the electronic energies of the products and the reactants at 0 K, ΔZPE is the difference in the zero-point energies of BH^+ and B, $\Delta E_{vib}(T)$ accounts for the change in the population of the vibrational levels at temperature *T*, and the last term incorporates the classical correction for translation ($^1/_2RT$ per degree of freedom), rotation ($1/2RT$ per degree of freedom), and the conversion factor of energy to enthalpy (ΔnRT).

3. Results

3.1. Determination of Thermodynamic Parameters for the Hydrogen-Bonding Formation between TA and Tertiary Amide Using the NIR Spectrum. We chose the ν^{as}_{N-H} + amide II combination band of TA to investigate the hydrogen-bonding formation between TA and tertiary amide, since this band has a large absorption coefficient and little interference from other peaks.[24] The ν^{as}_{N-H} + amide II combination bands of 8.0 mM TA with 40.0 mM DMA in CCl_4 at various temperatures are shown in Figure 1A. The peaks at 1968 nm

TABLE 1: Equilibrium Constants and Thermodynamic Parameters for the Hydrogen-Bonding Formation of TA with DMF, DEF, DIF, DMA, DEA, and DIA in CCl_4 Solution

proton donor	proton acceptor	equilibrium constant						ΔH° (kJ/mol)	ΔS° (J/(mol K))
		278 K	288 K	298 K	308 K	318 K	328 K		
TA	DMF	105.9	80.2	62.0	48.2	36.7	30.2	−19.7 ± 0.5	−31.9 ± 1.0
	DEF	100.4	76.0	56.6	45.5	35.7	37.2	−19.6 ± 0.5	−32.0 ± 1.0
	DIF	106.4	72.4	60.5	44.6	36.9	29.2	−19.3 ± 0.3	−30.9 ± 0.5
	DMA	116.5	84.4	64.9	50.8	38.8	31.2	−18.9 ± 0.2	−28.9 ± 0.5
	DEA	104.9	79.9	56.0	45.2	37.6	27.3	−19.3 ± 0.2	−31.1 ± 0.2
	DIA	90.3	70.3	49.5	39.3	31.1	25.2	−19.8 ± 0.3	−33.6 ± 0.6

(5081 cm^{-1}) and 1978 nm (5056 cm^{-1}) are assigned to monomeric TA and hydrogen-bonded TA, respectively. As the temperature increases, the absorption intensity of monomeric band increases, but that of the hydrogen-bonded band decreases. The spectra show an isosbestic point, which indicates the equilibrium of only two species, monomeric and hydrogen-bonded TA. In the temperature range between 278 and 328 K, the formation of 1:2 hydrogen-bonded complexes was not found. Each of monomeric and hydrogen-bonded TA absorption bands is well fitted by a Gaussian−Lorentzian product function, as shown in Figure 1B. The sum of two band areas is found to be independent of temperature within experimental error, indicating that the integrated absorption coefficients of monomer and complex bands are the same.

We noticed a shoulder on the ν^{as}_{N-H} + amide II combination band of TA/CCl_4 at about 1971 nm. After deconvoluting the band by Gaussian−Lorentzian product functions, we found a weak band whose area always occupies 22.7% of the total band area, independently of the temperature and concentration of TA. Since this unknown band appears at the same position of the hydrogen-bonded band, we corrected the hydrogen-bonded band by subtracting this band.[21−23] We found that self-association of TA is negligible until the concentration of 8 mM in the temperature range of 278−328 K.

The equilibrium of hydrogen bond formation and its equilibrium constants (K) are expressed by following equations:

$$\text{TA} + \text{acceptor} \leftrightarrow \text{TA:acceptor}$$

$$K = C_{1:1}/C_{\text{mono}}C_{\text{free}} \quad C_{1:1}/C_{\text{mono}} = C_{\text{free}}K \qquad (1)$$

where $C_{1:1}$ is the concentration of the hydrogen-bonded TA, C_{mono} is the concentration of monomeric TA, and C_{free} is the concentration of the free proton acceptors. The ratio of $C_{1:1}$ to C_{mono} is obtained directly from the area of two resolved bands, since the integrated absorption coefficients of two bands are the same. The linear fit for $C_{1:1}/C_{\text{mono}}$ vs C_{free} plot yields the equilibrium constant (K). Instead of using activity, the concentration was used as an approximation. Table 1 lists the equilibrium constants for the formation of 1:1 hydrogen-bonded complex in the temperature range 278−328 K. The equilibrium constants at 298 K are 62 ± 5, 57 ± 5, 61 ± 5, 65 ± 5, 56 ± 5, and 50 ± 5 M^{-1} for DMF, DEF, DIF, DMA, DEA, and DIA, respectively.

Thermodynamic parameters can be calculated from the van't Hoff equation, $(\ln K)/\mathrm{d}(1/T) = -\Delta H°/R$. The R ln K vs $1/T$ plots are shown in Figure 2. The values of thermodynamic parameters are listed in Table 1. The $\Delta H°$ values for the formation of the 1:1 hydrogen-bonded complex are −19.7 ± 0.5, −19.6 ± 0.5, and −19.3 ± 0.3 kJ/mol, for DMF, DEF, and DIF, respectively. The $\Delta H°$ values are −18.9 ± 0.3, −19.3 ± 0.3, and −19.8 ± 0.3 kJ/mol, respectively, for DMA, DEA, and DIA, showing an increase with the size of alkyl group. It is noted that the alkyl substituent effect on the equilibrium constant and $\Delta H°$ value is almost negligible in the formamide series, compared to the acetamide series. DMF can form a more stable hydrogen-bonded complex with TA than DMA, but the equilibrium constant of DMF is slightly smaller than that of DMA.

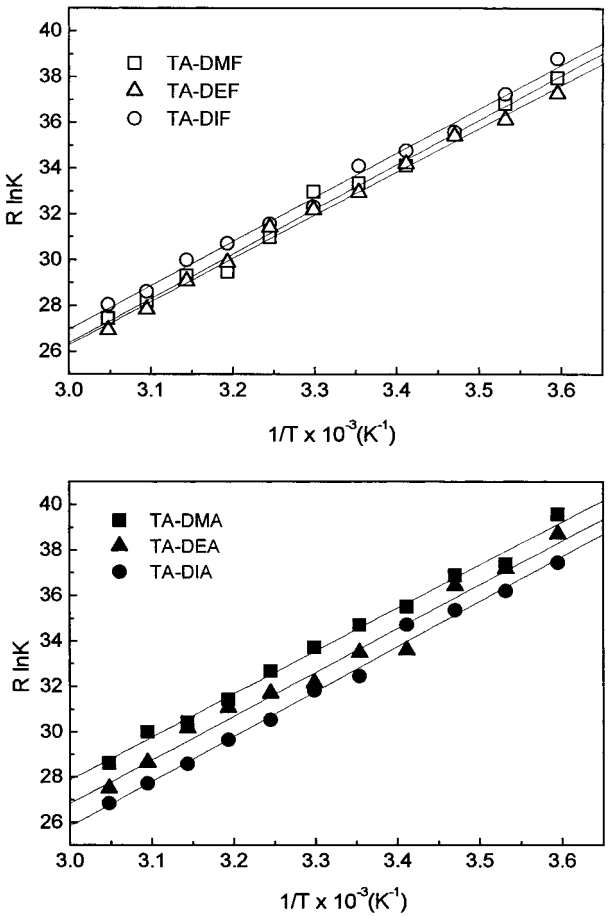

Figure 2. Plot of R ln K vs $1/T$ for the formation of 1:1 TA:*N*,*N*-dialkylacetamide hydrogen-bonded complexes.

3.2. IR Spectrum for the N−H Stretching Vibration. The IR absorption bands of TA at the N−H stretching vibration region, 3050−3550 cm^{-1}, have been measured. Figure 3A shows the IR spectrum of 3.0 mM TA with 18.0 mM DMF, DEF, and DIF, and Figure 3B is that with DMA, DEA, and DIA, in CCl_4 at 298 K. Each peak has been assigned as follows.[31,32] Peak 1 is the NH_2 asymmetric stretching of free TA, peak 2 is the NH_2 asymmetric stretching of the 1:1 TA:amide complex, and peak 3 is the NH_2 symmetric stretching of free TA. Peaks 4 and 5 resulted from the Fermi mixed resonance between symmetric N−H stretching and overtone of NH_2 bending of the 1:1 TA−amide complex.

Free TA peaks 1 and 3 did not shift at 3506 and 3390 cm^{-1}, respectively. However, TA−amide complex peaks 2, 4, and 5 are influenced by the proton acceptors. In the presence of DMF, DEF, and DIF, the positions of peak 4 are 3310, 3310, and 3307

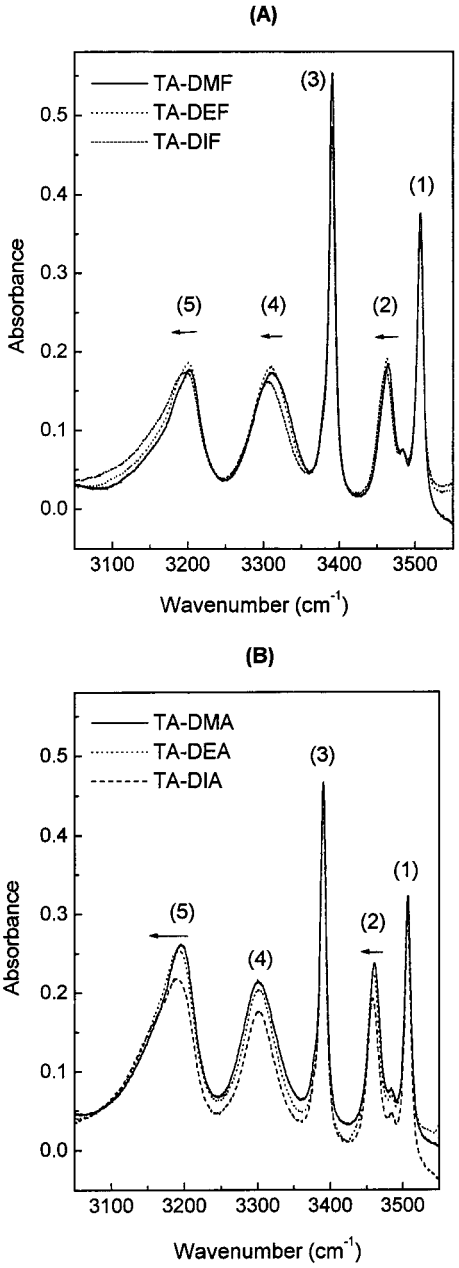

Figure 3. IR spectrum of 3.0 mM TA with 18.0 mM (A) DMF, DEF, and DIF and (B) DMA, DEA, and DIA in CCl_4 at 298 K.

cm^{-1} and those of peak 5 are 3202, 3200, and 3199 cm^{-1}, respectively. Therefore, the difference (Δ) of peaks 4 and 5 is 108, 109, and 108 cm^{-1} for DMF, DEF, and DIF, respectively, which is almost unchanged. The intensities of peaks 2, 4, and 5 also remain almost the same. In the presence of DMA, DEA, and DIA, the positions of peak 4 are 3300, 3302, and 3302 cm^{-1} and those of peak 5 are 3196, 3192, and 3199 cm^{-1}, respectively. The Δ values are 105, 110, and 112 cm^{-1} for DMA, DEA, and DIA, respectively, showing an increase with the size of alkyl group. It is noticed that the intensity of these three peaks decreases as the alkyl size increases. The results are summarized in Table 2.

3.3. Temperature Dependence of the ^{1}H NMR Chemical Shifts of TA. We measured the ^{1}H NMR chemical shift for N−Hs of TA as a function of temperature. Since TA has the internal rotational barrier around C−N bond as 17.3 kcal/mol,[19] two protons of TA resonate at 7.03 and 6.43 ppm for 3 mM TA/CCl_4 solution at room temperature (298 K). The NIR data have proved that TA is in free form under our experimental conditions. In amide, it is known that the proton syn (*syn*-H) to the carbonyl oxygen experiences the greater shielding and thus resonates at the higher field than the proton anti (*anti*-H) to the carbonyl oxygen.[33] Consistently, the downfield and upfield signals of TA can be assigned to *anti*-H and *syn*-H to the sulfur atom, respectively. Since TA is the stronger acid than acetamide,[34] free N−Hs of TA resonate downfield relative to those of amide that resonate around 6 ppm in noncompetitive solvent, e.g. CH_2Cl_2 and $CHCl_3$.[35] The temperature dependence of chemical shift ($\Delta\delta/\Delta T$) was measured as −5.6 and −2.0 ppb/K at the temperature of 283−313 K, for *anti*-H and *syn*-H, respectively, as shown in Figure 4.

TABLE 2: N−H Stretching IR Band Position of 1:1 TA:Amide Hydrogen-Bonded Complex for 3.0 mM TA/18.0 mM *N,N*-Dialkylamides/CCl_4

proton donor−proton acceptor	IR peak position (cm^{-1})			
	ν_2	ν_4	ν_5	$\Delta\nu^a$ (cm^{-1})
TA−DMF	3464	3310	3202	108
TA−DEF	3463	3310	3201	109
TA−DIF	3461	3307	3199	108
TA−DMA	3461	3300	3196	104
TA−DEA	3460	3302	3192	110
TA−DIA	3458	3302	3190	112

[a] $\Delta\nu = \nu_4 - \nu_5$ (cm^{-1}), the difference between the peak positions of ν_4 and ν_5, in cm^{-1}.

For 1:5 TA:amide solutions, the chemical shifts of *anti*-H and *syn*-H have been measured. In the presence of DMA, DEA, and DIA, *anti*-H resonates at 7.68, 7.74, and 7.76 ppm and *syn*-H resonates at 7.61, 7.57, and 7.51 ppm, respectively, at 298 K. As the alkyl group becomes bulky, *anti*-H and *syn*-H shift to the downfield and to the upfield, respectively, as shown in Figure 4A. The $\Delta\delta/\Delta T$ values of *anti*-H are −17.7, −19.2, and −21.6 ppb/K, respectively, for DMA, DEA, and DIA, showing an increase as the size of alkyl group increases. The $\Delta\delta/\Delta T$ value of *syn*-H is about −8 ppb/K, which is less than that of *anti*-H. The $\Delta\delta/\Delta T$ values of two N−Hs are much larger than those of free TA. The $\Delta\delta/\Delta T$ values are listed in Table 3.

For TA:DMF solution, the chemical shifts of two N−Hs are 7.46 and 7.35 ppm at 298 K. As the temperature increases, the separation of two peaks becomes larger, as shown in Figure 4B. As the temperature decreases to 283 K, two peaks merge into one peak. The $\Delta\delta/\Delta T$ values are measured as −9.5 and −16.7 ppb/K for the downfield and upfield peaks, respectively. Since the $\Delta\delta/\Delta T$ value of *anti*-H is always larger than that of *syn*-H in TA:acetamide solutions, it is reasonable to assign the downfield and upfield peaks to *syn*-H and to *anti*-H, respectively. In the case of DEF, a coalescent peak at 7.4 ppm starts splitting into two peaks as the temperature increases from 298 K. The $\Delta\delta/\Delta T$ values of *syn*- and *anti*-Hs are −10.0 and −16.2 ppb/K, respectively. For DIF, a coalescent peak also splits into two peaks as the temperature increases from 298 K. As the temperature decreases to 288 K, the peak splits again. The downfield and upfield peaks at the temperature of 308−318 K can be correlated with the upfield and downfield peaks at 283−288 K, respectively, providing the $\Delta\delta/\Delta T$ value as −11.1 ppb/K for *syn*-H and −17.2 ppb/K for *anti*-H.

A striking result is that in the presence of DMF, DEF, and DIF the peak of syn-H appears at the downfield relative to *anti*-H after the coalescent peak splits. As the alkyl size increases, the $-\Delta\delta/\Delta T$ values of both *anti*-H and *syn*-H increase. In the case of acetamide series, however, only the $-\Delta\delta/\Delta T$ value of *anti*-H increases as the alkyl group becomes bulky. The sum of $\Delta\delta/\Delta T$ values of *anti*- and *syn*-Hs is −26.2, −27.4,

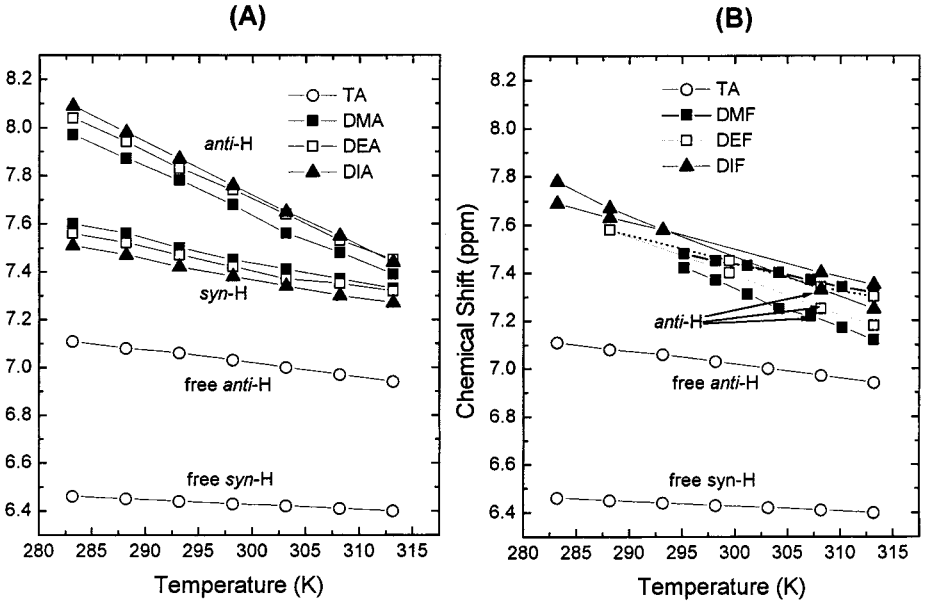

Figure 4. Plot of chemical shift (in ppm) of *anti*-H and *syn*-H of 8.0 mM TA as a function of temperature. The proton acceptors are 40.0 mM (A) DMF, DEF, and DIF and (B) DMA, DEA, and DIA. Data points are connected with a line.

TABLE 3: $\Delta\delta/\Delta T$ (ppb/K) values of 3.0 mM TA/CCl_4 and 8.0 mM TA/40.0 mM *N,N*-Dialkylamides/CCl_4

	$\Delta\delta/\Delta T$[a]			$\Delta\delta/\Delta T$[a]	
acceptors	H_{anti}	H_{syn}	acceptors	H_{anti}	H_{syn}
TA[b]	−5.6	−2.0	DMA	−19.6	−9.1
DMF	−16.7	−9.5	DEA	−19.9	−8.3
DEF	−16.6	−10.8	DIA	−21.6	−8.1
DIF	−17.2	−11.1			

[a] In units of ppb/K. [b] Proton donor.

and −28.3 ppb/K, respectively, for DMF, DEF, and DIF. The sum of $\Delta\delta/\Delta T$ values of *anti*- and *syn*-Hs is −26.3, −27.5, and −29.7 ppb/K for DMA, DEA, and DIA, respectively, showing a more pronounced increase with the alkyl group size, relative to the formamide series.

3.4. Proton Affinity (PA). We were only concerned about the PA values of *N,N*-dialkylamides for the oxygen site. The PA values of DMF, DEF, DIF, DMA, DEA, and DIA, at HF/6-31+G*, HF/6-31G**, and B3LYP/6-31G** levels, are listed in Table 4. Three different level calculations reveal consistently that there is an increase of PA as the alkyl group becomes bulky, for both the formamide and acetamide series. The PA value of DMA is larger than that of DMF.

The optimized geometry using the B3LYP/6-31G** level shows that the amide group of *N,N*-dialkylformamide is almost in a plane. However, for DMA, DEA, and DIA, the torsional angle of $\phi_1(R_2CNR_3)$ is 0.1, 2.0, and 3.7° and that of $\phi_2(OCNR_4)$ is −0.1, 0.3, and 1.2° (R_3 and R_4 are anti and syn to the carbonyl oxygen, respectively), respectively. The torsional angle increases as the alkyl size increases. For the protonated form of formamides and acetamides, the optimized geometry of amide group is almost planar.

4. Discussion

The thermodynamic data of hydrogen-bonded complex formation of DMF, DEF, and DIF with TA are almost the same. For DMA, DEA, and DIA, however, as the electron-donating ability of the alkyl group increases, the enthalpy change increases and the equilibrium constant decreases. The enthalpy change of the TA:DMA complex formation is less than that of TA:DMF, indicating that the electron-donating ability of the methyl group attached to the carbonyl carbon cannot simply enhance the stability of the hydrogen-bonded complex. In the acetamide series, the result that the equilibrium constant decreases as the alkyl size increases can be understood in terms of the entropy effect. More bulky alkyl group would restrict the hydrogen-bonding formation and thus increase the negative entropy.

Pawelka et al. measured the enthalpy change for the phenol−DMF complex formation in CCl_4 as −23.9 kJ/mol.[36] Since phenol is the stronger acid than TA, the phenol−DMA complex must be more stable than TA:DMA hydrogen-bonded complex, which agrees with our results. Hansen and Swenson reported the similar thermodynamic data for H_2O−DMF and H_2O−DMA hydrogen-bonding formation in CCl_4 as $\Delta H° = -13.4$ kJ/mol and $\Delta H° = -13.3$ kJ/mol, respectively.[3] For I_2−amide complex formation in CCl_4 solution, it is found that the enthalpy change of DMF, DMA, and DMP is −25.5, −26.8, and −26.8 kJ/mol, respectively, showing a slight increase with the alkyl size.[4] All of these experimental results indicate that the alkyl substitution to the carbonyl carbon cannot significantly enhance the hydrogen-bonding stability of amide.

The IR data of TA:formamide complexes show that the peak position and the Δ value of hydrogen-bonded Fermi-mixed N−H stretching peaks are not significantly changed as the size of alkyl group increases. However, in the acetamide series, as the alkyl group becomes bulky, the peaks shift to the lower frequency region and the Δ value increases obviously by 8 cm^{-1}. These results are consistent with the $-\Delta H°$ data obtained from the NIR spectrum. The Δ value of TA:DMF is larger than that of TA:DMA, which is also consistent with the NIR data that DMF shows a higher $-\Delta H°$ value.

The intensity of hydrogen-bonded Fermi-mixed N−H stretching peaks correlates with the equilibrium constant. For DMF, DEF, and DIF, the intensity remains almost the same. In the acetamide series, the intensity of these peaks decreases as the alkyl size increases, indicating a decrease of equilibrium constant. Therefore, we definitely conclude that there is a more pronounced alkyl substitutent effect on the hydrogen-bonding formation of acetamides, relative to formamides.

The $\Delta\delta/\Delta T$ values of free TA are −5.6 and −2.0 ppb/K, respectively, for *anti*-H and *syn*-H, in the temperature range

TABLE 4: Total Electronic Energy (E_{elec}), Zero-Point Energy (ZPE) of the *N,N*-Dialkylamide and Its Protonated Form, and Proton Affinity of *N,N*-Dialkylamide

	B3LYP/6-31G**			HF/6-31G**			HF/6-31+G*		
molecule	E_{elec} (hartree)	ZPE (hartree)	PA (kcal/mol)	E_{elec} (hartree)	ZPE (hartree)	PA (kcal/mol)	E_{elec} (hartree)	ZPE (hartree)	PA (kcal/mol)
DMF	−248.521 659	0.102 636	213.92	−247.002 139	0.109 745	217.15	−246.997 735	0.110 166	210.09
$DMFH^+$	−248.876 164	0.116 239		−247.362 807	0.124 362		−247.347 043	0.124 672	
DEF	−327.158 291	0.159 851	217.73	−325.081 454	0.170 607	220.37	−325.071 123	0.171 233	213.45
$DEFH^+$	−327.518 914	0.173 506		−325.447 233	0.185 207		−325.425 791	0.185 745	
DIF	−405.789 979	0.216 029	221.32	−403.154 090	0.230 421	223.65	−403.137 787	0.231 285	216.86
$DIFH^+$	−406.156 361	0.229 715		−403.524 978	0.244 904		−403.497 790	0.245 707	
DMA	−287.842 507	0.130 353	220.58	−286.044 468	0.139 331	223.04	−286.036 968	0.139 901	216.07
$DMAH^+$	−288.207 527	0.143 859		−286.414 219	0.153 646		−286.395 590	0.154 191	
DEA	−366.479 703	0.187 794	223.95	−364.124 226	0.200 391	225.89	−364.110 705	0.201 167	219.08
$DEAH^+$	−366.849 989	0.201 185		−364.498 506	0.214 691		−364.474 081	0.215 424	
DIA	−445.104 782	0.244 754	225.66	−442.187 750	0.261 015	227.32	−442.168 410	0.262 093	220.72
$DIAH^+$	−445.477 680	0.258 041		−442.564 353	0.275 359		−442.534 519	0.276 460	

283−313 K. The $\Delta\delta/\Delta T$ values of free amide N−Hs are usually rationalized by the torsional oscillations at the C−N bond that increase in amplitude upon warming.[37] Since the rotational barrier of TA is higher than that of amide,[19] the temperature dependence of torsional vibration is expected to be less in TA. In the presence of proton acceptors, the $\Delta\delta/\Delta T$ value would be more influenced by the intermolecular hydrogen-bonding interaction.

The chemical shift of ^{1}H NMR can provide a detailed insight how *anti*-H and *syn*-H of TA can form the hydrogen bonding with tertiary amides. The $\Delta\delta/\Delta T$ value of *anti*-H was measured as −17.7, −19.2, and −21.6 ppb/K in the presence of DMA, DEA, and DIA, respectively, which is much greater than that of *syn*-H (−8 ppb/K). These results indicate that TA:acetamide complex formation through *anti*-H of TA is more stable than that via *syn*-H, and the alkyl substituents stabilize preferentially the hydrogen-bonded complex formed via *anti*-H.

For TA:formamide complex formations, the $\Delta\delta/\Delta T$ values of *anti*-H and *syn*-H are greater than −8 ppb/K and the *syn*-H resonates at downfield after the coalescence temperature around 290−300 K. These results indicate the hydrogen-bonding formation via *syn*-H also takes place as well as that via *anti*-H. Since formamides lack of methyl group attached to the carbonyl group, we can expect less steric hindrance in the hydrogen-bonding formation through *syn*-H, relative to acetamides. The $\Delta\delta/\Delta T$ value of *anti*-H is higher than that of *syn*-H, indicating that the hydrogen-bonded complex via *anti*-H is still more stable than that of *syn*-H. The hydrogen bonding via *syn*-H may contribute to enhancing the enthalpy change, which results in higher enthalpy change of DMF compared to DMA. Furthermore, the hydrogen bonding via *syn*-H may lead all three formamides to show similar enthalpy changes and equilibrium constants.

The hydrogen-bonding ability of tertiary amides can be compared with ab initio PA values.[38] As the alkyl group becomes bulky, the PA value increases for both formamide and acetamide series. The PA values are enhanced by the alkyl substitution to the carbonyl carbon more than that to the nitrogen atom. In the acetamide series, there is a linear correlation between the PA value and the enthalpy change of the hydrogen-bonded complex formation. However, the experimental results that the enthalpy change of DMF is higher than that of DMA and there is no enthalpy difference among the formamide series are inconsistent with the PA values. The PA calculations adopt the same type of proton for all amides. If formamide forms the hydrogen bond via *syn*-H of TA, as we suggested from the NMR data, the PA value might not predict precisely the enthalpy change of hydrogen-bonding formation.

Wiberg et al. describes why the C−N rotational barrier of DMF is higher than that of DMA, by using the ground-state methyl−methyl repulsive interaction of DMA.[13] True et al. reported the gas-phase ^{1}H NMR studies for the rotational barrier and the stability of symmetric and asymmetric *N,N*-dialkylamide conformers.[7−12] They suggested that an inability to accommodate the larger subsitutents in the amide plane results in a loss of resonance stabilization in the ground state and a lower rotational barrier. The rotational barriers of DMA and DIA in gas phase were found to be 15.7 and 14.3 kcal/mol, respectively. The rotational barrier was measured as 19.8, 19.2, and 19.1 kcal/mol, respectively, for DMF, DEF, and DIF in gas phase.[11] Therefore, the alkyl effect on the rotational barrier is more pronounced in the acetamide series than in the formamide series. We can correlate the rotational barriers with the equilibrium constants of hydrogen-bonding formation. The larger repulsion between the alkyl substituents will result in severe steric hindrance for the hydrogen-bonding interaction with TA and, thus, reduce the equilibrium constant of hydrogen-bonding formation. Therefore, the alkyl substituent effect would be more pronounced in acetamides, compared to formamides.

5. Conclusions

We have studied the hydrogen-bonding formation of symmetric *N,N*-dialkyl-substituted formamides such as DMF, DEF, and DIF and *N,N*-dialkyl-substituted acetamides such as DMA, DEA, and DIA with TA in CCl_4. The NIR, IR, and proton NMR spectroscopic techniques were employed. We performed ab initio quantum mechanical calculations for the proton affinity of these tertiary amides. The NIR and IR data show that, in the acetamide series, the stability of the TA:amide 1:1 hydrogen-bonded complex increases as the alkyl group becomes bulky. However, in the formamide series, the alkyl substitution cannot enhance the stability of the hydrogen-bonding complex as much as that of acetamide series. The PA value of acetamides shows a better correlation with the enthalpy change of hydrogen-bonded complex formation than that of formamides. We measured the temperature dependence of chemical shift for *anti*-H and *syn*-H of TA. It is found that the temperature dependence of *syn*-H is larger in the presence of formamides than acetamides. This suggests more possibility of hydrogen-bonding formation via *syn*-H of TA for formamides than acetamides, due to less steric hindrance.

Acknowledgment. We wish to acknowledge the financial support of the Korea Research Foundation made in the program year of 1998.

References and Notes

(1) Kollman, P. *Chem. Rev.* **1993**, *93*, 2395−2417.
(2) Le Questel, J.-Y.; Laurence, C.; Lachkar, A.; Helbert, M.; Berthelot, M. *J. Chem. Soc., Perkin Trans. 2* **1992**, 2091−2094.
(3) Hansen, D. B.; Swenson, C. A. *J. Phys. Chem*. **1973**, *77*, 2401−2406.
(4) Drago, R. S.; Wenz, D. A.; Carlson, R. L. *J. Am. Chem. Soc*. **1962**, *84*, 1106−1109.
(5) Wolfenden, R. *Biochemistry* **1978**, *17*, 201−204
(6) Morgantini, P.; Kollman, P. *J. Am. Chem. Soc*. **1995**, *117*, 6057−6063.
(7) Taha, A. N.; Neugebauer Crawford, S. M.; True, N. S. *J. Phys. Chem. A* **1998**, *102*, 1425−1430.
(8) Ross, B. D.; True, N. S. *J. Am. Chem. Soc*. **1984**, *196*, 2451−2452.
(9) Suarez, C.; Tafazzoli, M.; True, N. S.; Gerrard, S.; LeMaster, C. B.; LeMaster, C. L. *J. Phys. Chem*. **1995**, *99*, 8170−8176.
(10) Rabinovitz, M.; Pines, A. *J. Am. Chem. Soc.* **1969**, *91*, 1585−1589.
(11) LeMaster, C. B.; True, N. S. *J. Phys. Chem*. **1989**, *93*, 1307−1311.
(12) Neugebauer Crawford, S. M.; Taha, A. N.; True, N. S.; LeMaster, C. B. *J. Phys. Chem. A* **1997**, *101*, 4699−4706.
(13) Wiberg, K. B.; Rablen, P. R.; Rush, D. J.; Keith, T. A. *J. Am. Chem. Soc*. **1995**, *117*, 4261−4270.
(14) Adelsteinsson, H.; Maulitz, A. H.; Bruce, T. C. *J. Am. Chem. Soc*. **1996**, *118*, 7689−7693.
(15) Ou, M.-C.; Chu, S.-Y. *J. Phys. Chem*. **1995**, *99*, 556−562 and references therein.
(16) Lauvergnant, D.; Hilberty, P. C. *J. Am. Chem. Soc*. **1997**, *119*, 9478−9482.
(17) Wiberg, K. B.; Rablen, P. R. *J. Am. Chem. Soc*. **1995**, *117*, 2201−2209.
(18) Laidig, K. E.; Cameron, L. M. *J. Am. Chem. Soc*. **1996**, *118*, 1737−1742.
(19) Choe, Y. K.; Song, G. I.; Choi, Y.-S.; Yoon, C.-J. *Bull. Korean Chem. Soc*. **1997**, *18*, 1094−1099.
(20) Branden, C.; Tooze, J. *Introduction of Protein Structure*; Garland Publishing: New York and London, 1991; p 12.
(21) Choi, Y.-S.; Huh, Y. D.; Bonner, O. D. *Spectrochim. Acta* **1985**, *41A*, 1127−1133.
(22) Choi, Y.-S.; Kim, J. K.; Park, J.; Yu, J.-A.; Yoon, C.-J. *Spectrochim. Acta* **1996**, *52A*, 1779−1783.
(23) Min, B. K.; Lee, H.-J.; Choi, Y.-S.; Park, J.; Yoon, C.-J.; Yu, J.-A. *J. Mol. Struct.* **1998**, *471*, 283−288.
(24) Krikorian, S. E.; Mahpour, M. *Spectrochim. Acta* **1973**, *29A*, 1233−1246.
(25) Gellman, S. H.; Adams, B. R.; Dado, G. P. *J. Am. Chem. Soc.* **1990**, *112*, 460−461.
(26) Gellman, S. H.; Dado, G. P.; Liang, G.-B.; Adams, B. R. *J. Am. Chem. Soc*. **1991**, *113*, 1164−1173.
(27) Frisch, M. J.; Trucks, G. W.; Schlegel, H. B.; Gill, P. M. W.; Johnson, B. G.; Robb, M. A.; Cheeseman, J. R.; Keith, T.; Petersson, G. A.; Montgomery, J. A.; Raghavachari, K.; Al-Laham, M. A.; Zakrzewski, V. G.; Ortiz, J. V.; Foresman, J. B.; Cioslowski, J.; Stefanov, B. B.; Nanayakkara, A.; Challacombe, M.; Peng, C. Y.; Ayala, P. Y.; Chen, W.; Wong, M. W.; Andres, J. L.; Replogle, E. S.; Gomperts, R.; Martin, R. L.; Fox, D. J.; Binkley, J. S.; Defrees, D. J.; Baker, J.; Stewart, J. P.; Head-Gordon, M.; Gonzalez, C.; Pople, J. A. *Gaussian 94*, Revision E.1; Gaussian, Inc., Pittsburgh, PA, 1995.
(28) Dewar, M. J. S.; Zoebisch, E. G.; Healy, E. F.; Stewart, J. J. P. *J. Am. Chem. Soc.* **1985**, *107*, 3902−3909.
(29) (a) Petersson, G. A.; Bennett, A.; Tensfeldt, T. G.; Al-Laham, M. A.; Shirley, W. A.; Mantzaris, J. *J. Chem. Phys.* **1988**, *89*, 2193−2218. (b) Petersson, G. A.; Al-Laham, M. A. *J. Chem. Phys.* **1991**, 94, 6081−6101.
(30) (a) Becke, A. D. *Phys. Rev. A* **1998**, *38*, 3098. (b) Lee, C.; Yang, W.; Parr, R. G. *Phys. Rev. B* **1988**, *37*, 785. (c) Baerends, E. J.; Gritsenko, O. V. *J. Phys. Chem.* **1997**, *101*, 5383−5403.
(31) Walter, W.; Vinkler, P. *Spectrochim. Acta*. **1977**, *33A*, 205−212.
(32) Vinkler, P.; Walter, W.; Keresztury, G. *Spectrochim. Acta* **1980**, *36A*, 935−940.
(33) Hollósi, M.; Thorsen, M.; Zewdu, M.; Ruff, F.; Kajtár, M.; Kövér, K. E. *Tetrahedron* **1986**, *42*, 3931−3942.
(34) Sandström, J. *J. Phys. Chem.* **1967**, *71*, 2318−2325.
(35) Chitnumsub, P.; Fiori, W. R.; Lashuel, H. A.; Diaz, H.; Kelly, J. W. *Bioorg. Med. Chem.* **1999**, *7*, 39−59.
(36) Pawelka, Z.; Zeegers-Huyskens, Th. *Vib. Spectrosc.* **1998**, *18*, 41−49.
(37) Haushalter, K. A.; Lau, J.; Roberts, J. D. *J. Am. Chem. Soc*. **1996**, *118*, 8891−8896.
(38) Rablen, P. R.; Lockman, J. W.; Jorgensen, W. L. *J. Phys. Chem. A* **1998**, *102*, 3782−3797